ASIA-PACIFIC JOURNAL OF ATMOSPHERIC SCIENCES, 44, 2, 2008, p. 121-135

Simulations of the Mesoscale Cyclone Accompanying the Storm Surge on 30 March 2007 in the Western Coast of Korea

Jeong-Wook Lee[1], Ki-Young Heo[1], Kyong-Hwan Seo[1], Kyung-Ja Ha[1], Kwang-Soon Park[2] and Ki-Cheon Jun[2]

[1]*Division of Earth Environmental System, Pusan National University*
[2]*Coastal Engineering Research Division, Korea Ocean Research & Development Institute*
(Manuscript received 24 December 2007; in final form 6 March 2008)

Abstract

Cyclones are quite common and occasionally are disastrous because of the location of the Korean Peninsula. The storm surge on 30 March 2007 was very unusual in terms of its presence on the western coast and in terms of typical mesoscale cyclone development. Very specific numbers for sea level pressure and sea surface wind are required to predict cyclone disaster potential in the Korean Peninsula. In this study, we attempt to reproduce the reliable surface wind and sea level pressure using optimal physical parameterizations for high wind conditions in different models such as MM5, WRF, and COAMPS. To select the optimal physics combinations for the high winds, we designed three experiments with different parameterization combinations for MM5 and WRF as follows; EXP1 (Eta PBL and Betts-Miller cumulus), EXP2 (Eta PBL and Grell cumulus) and EXP3 (MRF PBL and Kain-Fritsch cumulus). EXP2 showed good performance in terms of the distribution and the magnitude of wind speed. The WRF and MM5 with EXP2 physics have an early evolution and a delayed maximum magnitude, respectively. The COAMPS model simulated the evolution but with a smaller magnitude. Warm advection, moisture flux and its convergence, convective instability, and longitude-height cross-section of temperature were explored by MM5 and WRF with EXP2 and COAMPS.

Key words: Mesoscale cyclone, sea level pressure, sea surface wind, MM5, WRF, COAMPS

1. Introduction

Because the Korean Peninsula is located in the middle-latitude, generation and transit of cyclone frequently occurred and occasionally caused the disaster (Lee and Chang, 1997). Joung *et al*. (1984) showed that cyclones on the East Sea were associated with baroclinic waves and their development was followed by a decrease of atmospheric stability. Chen and Dell'Osso (1987) proved that latent heating had a profound impact on amplifying jet streak circulation and the vertical coupling within the systems, which appeared to prime for rapid cyclogenesis along the coast, and that the sensible heating contributed nearly 18% to the surface development. Lee *et al*. (1991) concluded that proper release of latent heat by a well-parameterized convective scheme could predict the development of cyclones and associated precipitation.

The sensitivity of model parameters and initial conditions required to accurately predict the development of an extratropical cyclone must now be explored. Orlanski and Katzfey (1987) evaluated the sensitivity of a model result with a one-way nested system to different parameters that may affect the forecast. They found that the most significant improvement in accuracy occurred when the horizontal resolution was increased. Lee and Hong (1989) suggested that the model can be improved by a proper parameterization of the surface conditions in the ocean area near the continent for improved simulation of winter cyclones. Lee and Chang (1997) showed that well-defined warm advection ahead of the lower tropospheric trough and cold advection be-

Corresponding Author: Kyung-Ja Ha, Division of Earth Environmental System, Pusan National University, 30 Jangjeon-dong, Geumjeong-gu, Busan 609-735.
Phone : +82-51-510-2177, Fax : +82-51-515-1689
E-mail: kjha@pusan.ac.kr

hind the system at initiation plays an important role in intensification of the cyclone.

In this study, we selected the optimal physics combinations for the high winds (Davis and Simon, 2001; Ivanov and Palamarchuk, 2007) in Fifth-generation Mesoscale Model (MM5) and Weather Research and Forecasting model (WRF) and examined the results between MM5, WRF and the Coupled Ocean/ Atmosphere Mesoscale Prediction System (COAMPS) for the evolution of surface wind and sea level pressure associated with a cyclone. Finally, we investigated the cause of cyclone development.

2. Case day

A mesoscale cyclone accompanied by high wind induced a surge on the southwestern coast of the Korean Peninsula on 30 March 2007. The storm surge occurred simultaneously with the high tide; the sea-surface height was recorded above the high water level culminating at 703 cm, which is corresponding to the additional sea-surface height of approximately 200 cm from the height of Yeonggwang (35.3°N, 126.5°E) high tide at 1631 UTC 30 March 2007. The maximum wind gust and wind speed reached 20 m s^{-1} and 16 m s^{-1}, respectively, up to 4 hours before the storm surge (Fig. 1).

Figure 2 shows the surface weather chart on 30 March 2007. On 0900 UTC 30 March 2007, a small scale cyclone and anticyclone were located in the Korean Peninsula (Fig. 2a). The quickly generated cyclone, as shown in the black box of Fig. 2b, of 1500 UTC 30 March 2007, was dissipated and the pattern of air pressure moved eastward on 2100 UTC 30 March 2007 (Fig. 2c). Usually, storm surges are the result of a typhoon over the east or south coasts of the Korean Peninsula. However, this case is exceptional, as it was a mesoscale cyclone with a center pressure of 1010 hPa at Yeonggwang near the southwestern coast of the Korean Peninsula (Fig. 2b). To produce an accurate cyclone that can cause disaster, it is necessary to calculate the wind speed over the ocean.

3. Models and experimental design

MM5 version 3.7, WRF version 2.2 and COAMPS version 3.1 were used in this study. The nested domains over the center of 35.0°N and 129.0°E were covered with 115 (in longitude) x 124 (in latitude) grids in the 27 km mesh and 175 (in longitude) x 238 (in latitude) grids in the 9 km mesh systems, respectively. Initial and boundary conditions were based on the National Centers for Environmental Prediction (NCEP) Final Analysis (FNL) for the MM5

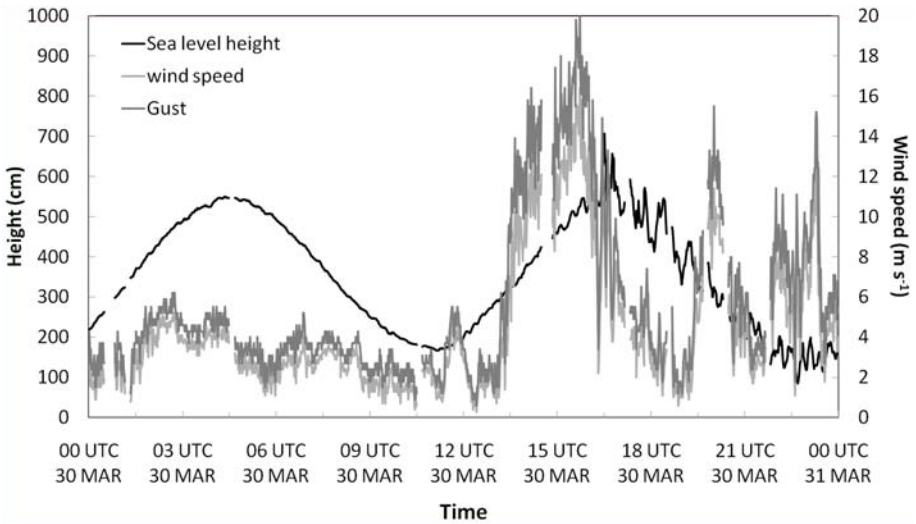

Fig. 1. Observed time series of sea level height (cm, black), wind speed (m s^{-1}, light grey) and the maximum wind gust (m s^{-1}, dark grey) at Yeonggwang (35.3°N, 126.5°E) from 00 UTC 30 to 00 UTC 31 March 2007.

(a) 0900 UTC 30 Mar. 2007

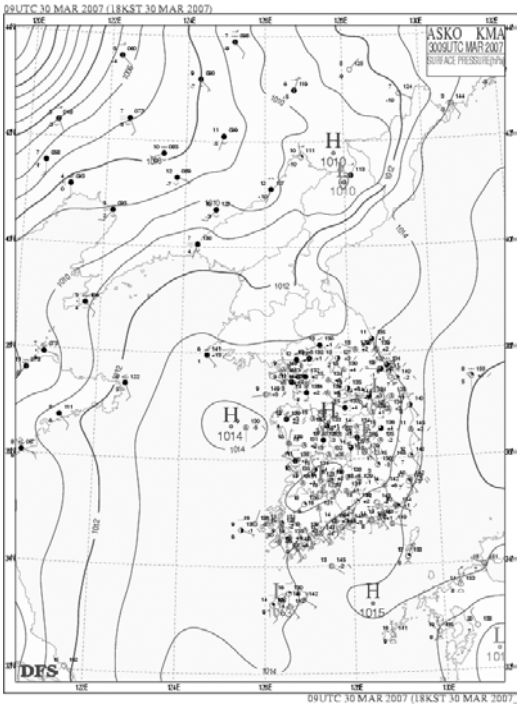

(b) 1500 UTC 30 Mar. 2007

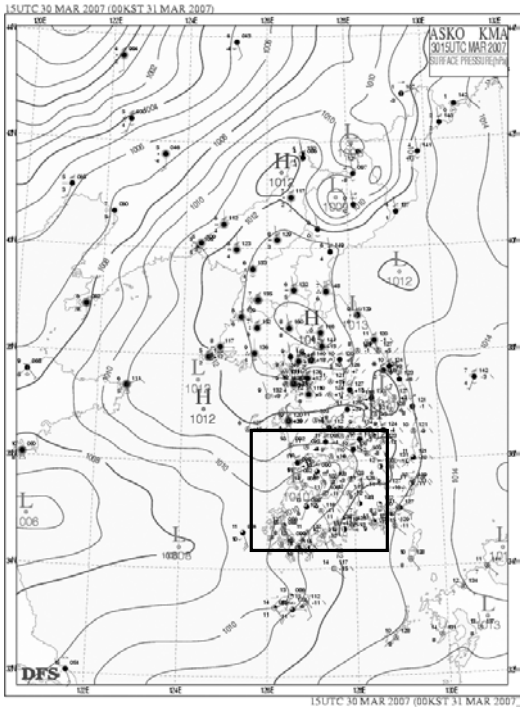

(c) 2100 UTC 30 Mar. 2007

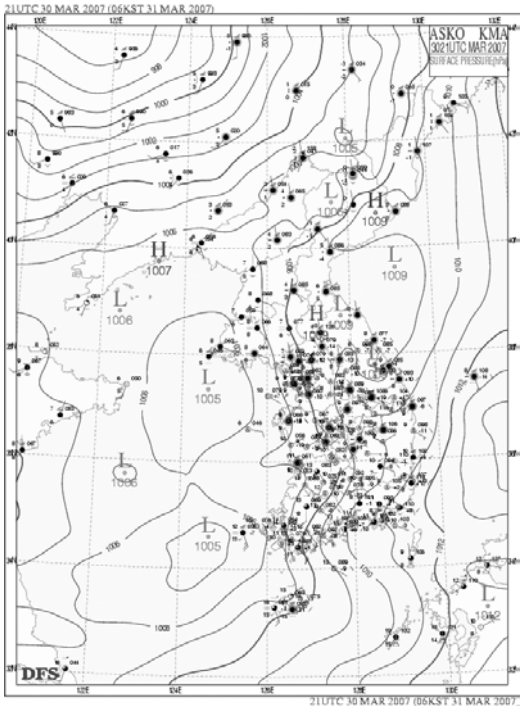

Fig. 2. Surface weather chart on (a) 0900 UTC 30 March 2007, (b) 1500 UTC 30 March 2007, and (c) 2100 UTC 30 March 2007.

Table 1. MM5, WRF and COAMPS model description.

Model configuration	MM5	WRF	COAMPS
Grid and nest	Arakawa-C Multiple nest	Arakawa-B Multiple nest	Arakawa-C Multiple nest
Vertical coordinate system	Sigma coordinate	(hybrid) sigma-z (pressure) - Terrain following	Sigma coordinate
Vertical resolution	27 levels		30 levels
Initial field and boundary condition	FNL (Final Analysis) data		NOGAPS data
Physical scheme	Simple ice scheme, RRTM / Simple MM5 scheme, 5-layer soil model		Explicit moist physics, Single layer model

and WRF. MM5 and WRF are non-hydrostatic, primitive-equation model with multiple-nesting capabilities to enhance the resolution over the area of interest. The initial and boundary conditions for the atmospheric component of COAMPS were the Navy Operational Global Atmospheric Prediction System (NOGAPS) and satellite data came from Geostationary Operational Environmental Satellites (GOES), Quick Scatterometer (QuikSCAT), Special Sensor Microwave/Imager (SSM/I). The simulations were executed from 0000 UTC 30 March 2007 to 0000 UTC 31 March 2007. Table 1 shows the configurations of MM5, WRF and COAMPS.

Except for the COAMPS model, three sets of experiments were carried out to select the physics options which could accurately simulate the magnitude and the evolution of the cyclone in high wind conditions (Table 2). To choice optimal physical parameterization schemes, many factors including simulated phenomenon, numerical model, model resolution and simulation region should be considered. However, it was difficult to choice the optimal physical parameterization schemes to simulate the present cyclone case. In the present case, an intense cyclone accompanied by the maximum wind gust of 20 m s^{-1} caused the storm surge. To simulate the intense cyclone, EXP1 and EXP2 were selected from the best physical parameterizations for tropical cyclone prediction accompanied by strong wind, which was suggested by Davis and Simon (2001). EXP3 came from the best optimal parameterization scheme sets to simulate atmospheric variables including air temperature, relative humidity and geopotential height using MM5 model (Ivanov and Palamarchuk, 2007).

The model physics parameterizations were identical for three sets except for the planetary boundary layer (PBL) and cumulus parameterization (CP). In the case of the PBL parameterization scheme, EXP1 and EXP2 used Eta PBL (Janjic, 1990; Mellor and Yamada, 1982) and EXP3 used MRF PBL (Hong and Pan, 1996). The MRF PBL scheme is a first-order, nonlocal K scheme, which includes counter-gradient transports of temperature and moisture that account for the contributions from large-scale eddies (Hong and Pan, 1996). The Eta PBL scheme is a Mellor – Yamada (1982) level-2.5 scheme, or a variant of 1.5-order closure model that includes a prognostic equation of the TKE. Zhang and Zheng (2004) re-

Table 2. Experimental designs for physics options.

Physics Options	EXP1	EXP2	EXP3
PBL Scheme	Eta	Eta	MRF
Cumulus Scheme	Betts-Miller	Grell	Kain-Fritsch
Explicit Moisture Scheme	Mixed phase		
Surface Scheme	Five-Layer Soil		
Radiation Scheme	RRTM longwave scheme		

ferred that these PBL schemes contained nonlocal treatments of the unstable PBL developments, which included TKE closures (Eta PBL), counter-gradient heat fluxes (MRF PBL). The model domain has (x, y) dimensions of EXP1, EXP2, and EXP3 used the Betts-Miller (Betts, 1986; Betts and Miller, 1993; Janjic, 1994) scheme, Grell (Grell *et al*., 1994) scheme, and Kain-Fritsch (Kain and Fritsch, 1993) schemes for the cumulus scheme, respectively. The physics parameterizations were mixed phase scheme (Reinsner *et al*., 1998) for the explicit moisture scheme, five-layer soil for the land surface model, rapid RTM (Mlawer *et al*., 1997) for long wave radiation and simple MM5 (Dudhia, 1989) for short wave radiation. The selected physics schemes were applied to the MM5 and WRF model and then the results are compared with the output of the COAMPS model.

4. Optimal combination of parameterization for MM5 and WRF

To select the optimal physics combination for the high wind, we executed three experiments with different parameterizations. Figure 3 shows the horizontal distribution of wind speed obtained by QuikSCAT. Observation recorded a strong wind region in the western part of Yellow Sea, South Sea and East Sea on 1012 UTC 30 March 2007 (Fig. 3a). On 2124 UTC 30 March 2007, the distribution of wind speed was stronger than that previously, especially in the East China Sea, Yellow Sea and East Sea (Fig. 3b).

To compare the distribution of wind speed obtained by model results with that obtained by QuikSCAT, Figures 4 and 5 show the horizontal distribution of the simulated sea surface wind speed at 1000 UTC and 2100 UTC 30 March 2007, respectively, using MM5 and WRF with different physics for Table 1. At 1000 UTC 30 March 2007, the strong wind speed was well simulated in all experiments over the western part of Yellow Sea and the east coast of the Korea although EXP3 showed that distribution of wind speed was weaker than EXP1 and EXP2 in the South Sea (Fig. 4). All experiments have a good performance to simulate the sea surface wind under relatively weak wind conditions

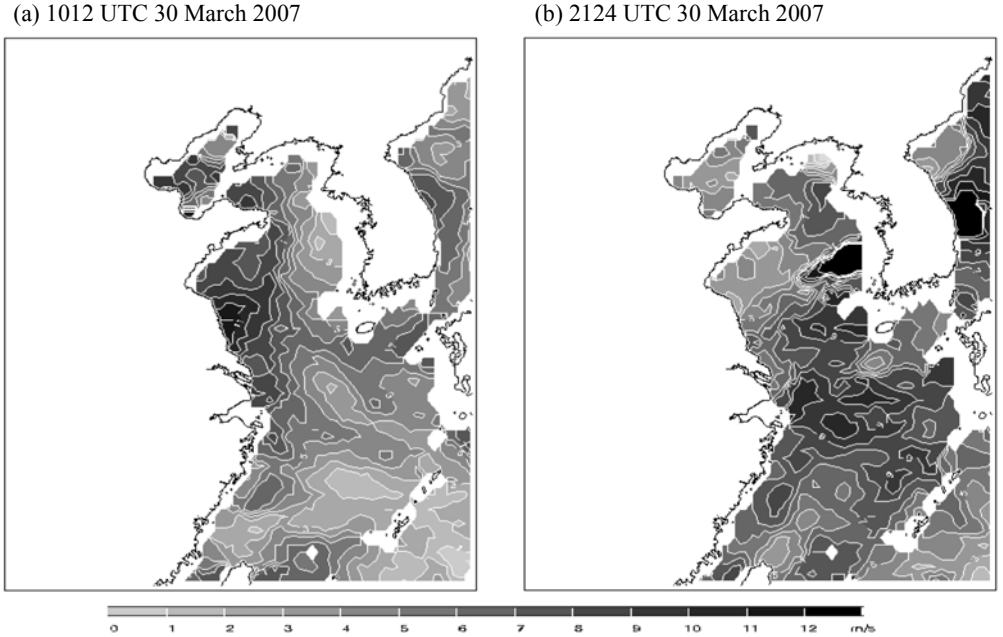

Fig. 3. Horizontal distribution of sea surface wind obtained by QuikSCAT on (a) 1012 UTC 30 March 2007 and (b) 2124 UTC 30 March 2007.

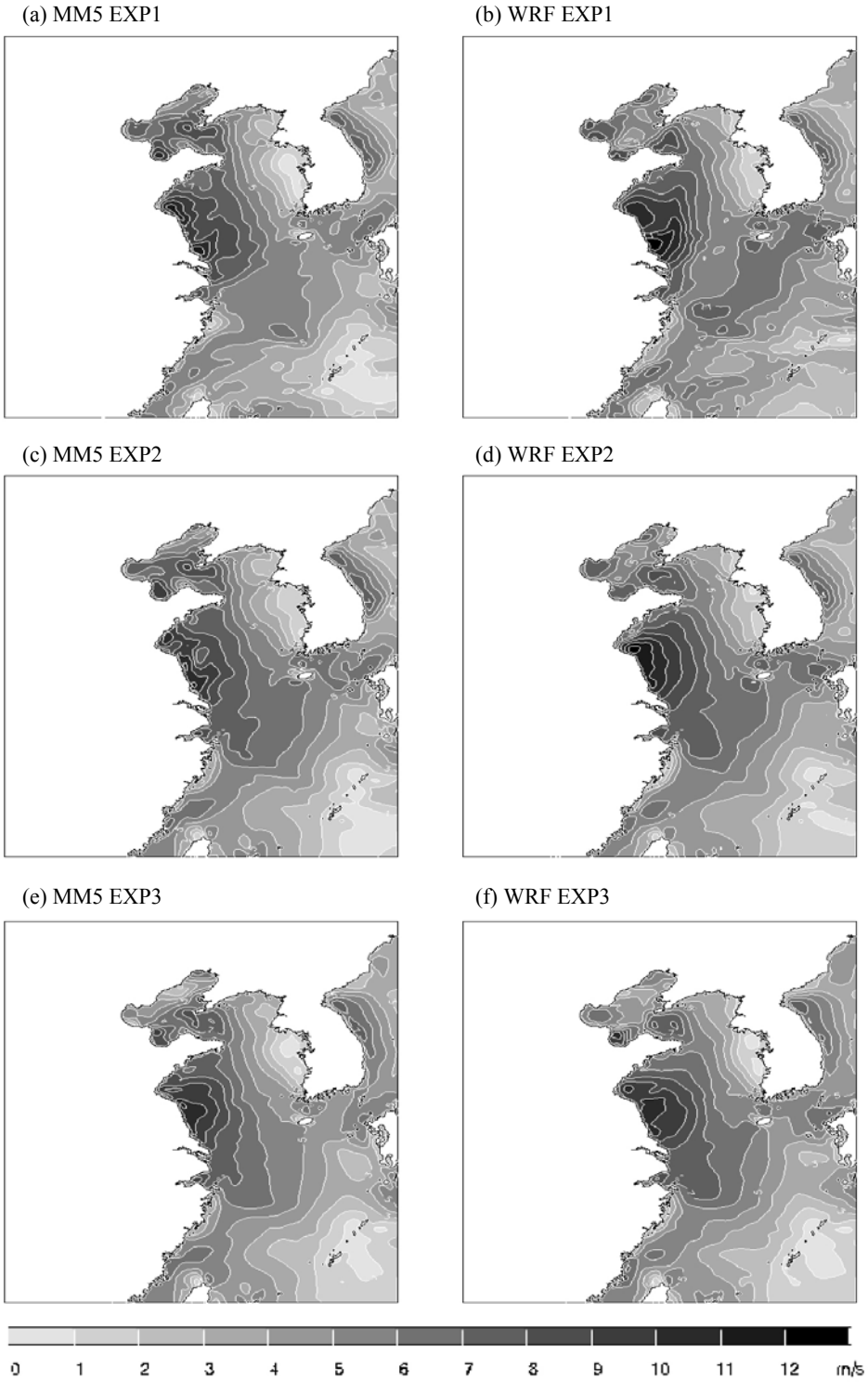

Fig. 4. Horizontal distribution of sea surface wind simulated by (a) MM5 EXP1, (b) WRF EXP1, (c) MM5 EXP2, (d) WRF EXP2, (e) MM5 EXP3 and (f) WRF EXP3 on 1000 UTC 30 March 2007.

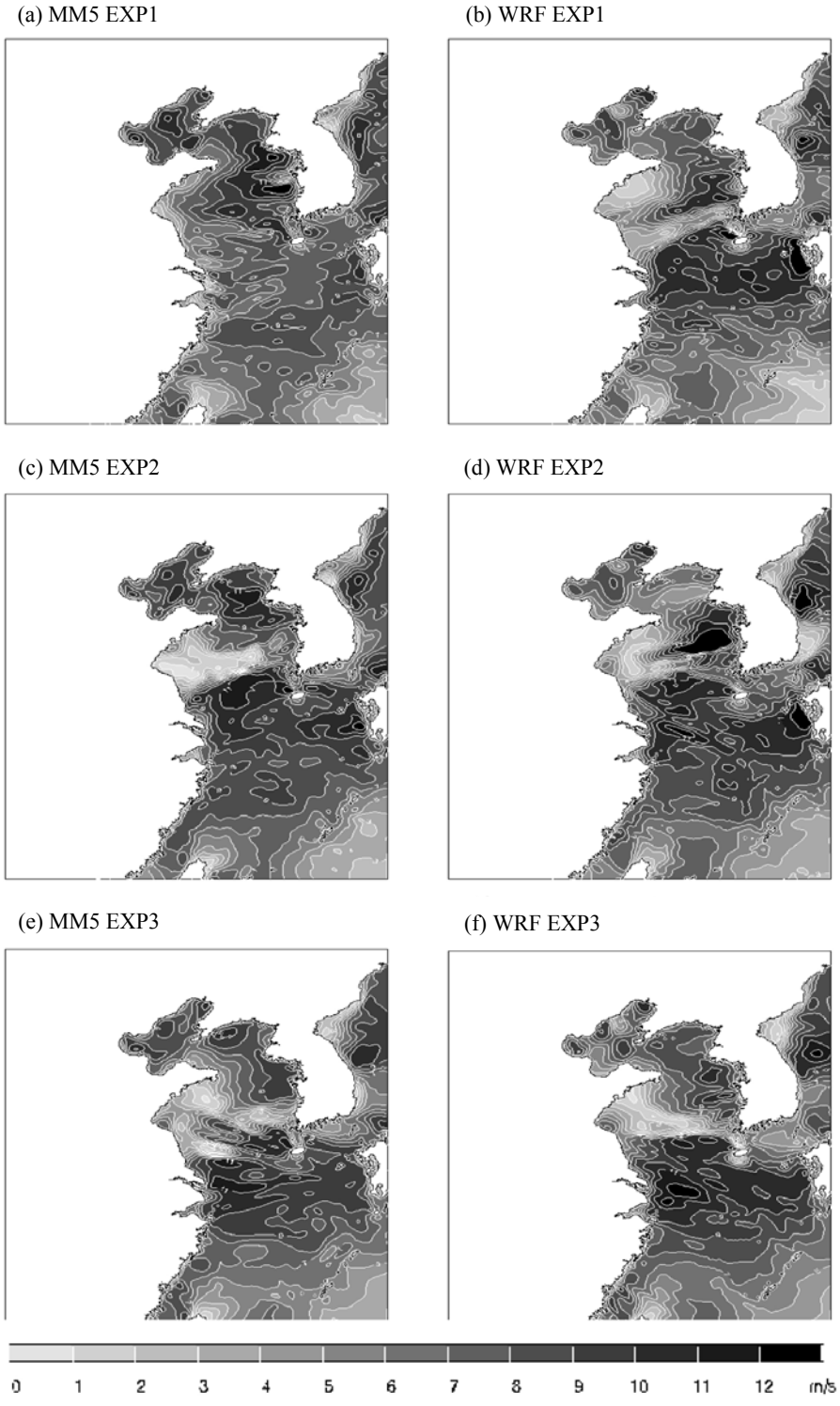

Fig. 5. Same as Fig. 4 except for 2100 UTC 30 March 2007.

(below 10 m s^{-1}). At 2100 UTC 30 March 2007, the model result for a strong wind region differed from each experiment (Fig. 5). MM5 simulations show the stronger wind over the northern part of the Yellow Sea, compared to the observation. Three experiments using MM5 tended to underestimate the wind speed or to misestimate the locations of strong wind region. All experiments produced strong wind regions in the East China Sea, the west coast and the east coast of the Korea except for the MM5 EXP1. EXP2 and EXP3 showed better distributions compared to the EXP1, even though the speeds in the western Korean Peninsula were underestimated. Overall, wind speed simulated by WRF was stronger than MM5.

In the WRF simulations, EXP2 properly simulated the locations of strong wind region and the wind speed above 12 m s^{-1} while EXP1 and EXP3 tended to underestimate the wind speed. Among the results of experiments using both models, simulated maximum winds varied by about 13 m s^{-1} with the Eta PBL schemes producing the stronger wind and the MRF PBL scheme producing the weaker wind. This result was found to the difference between the MRF and the

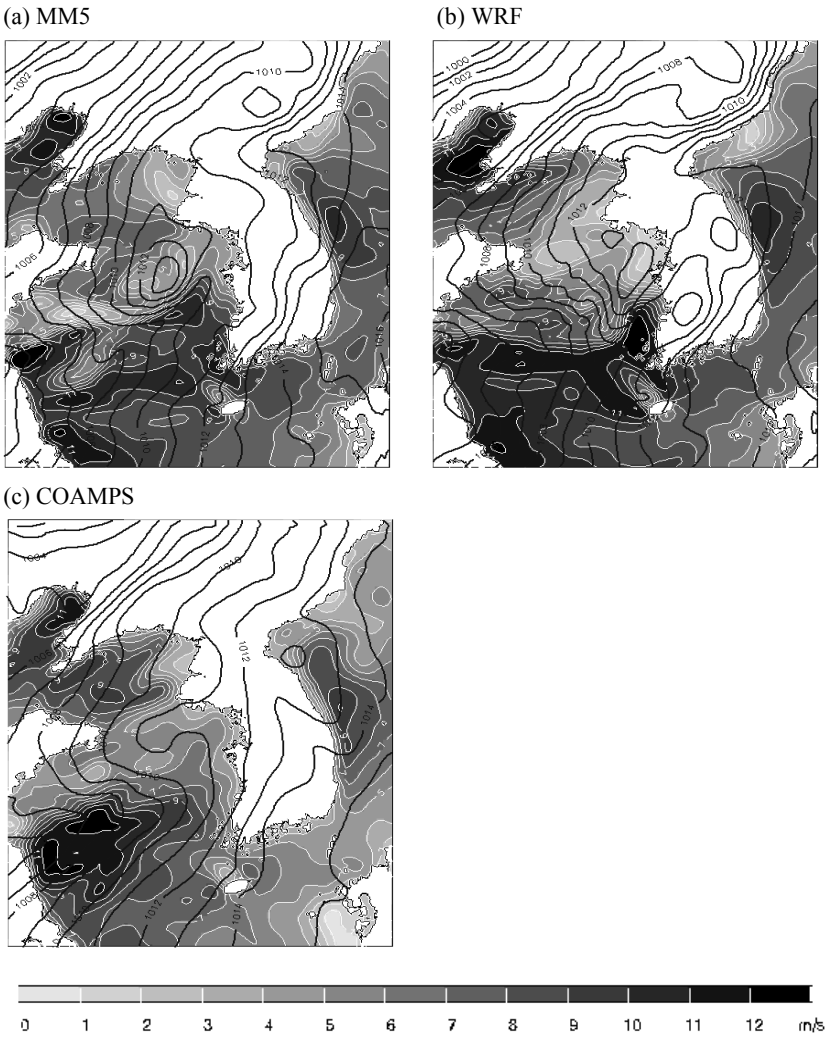

Fig. 6. Horizontal distribution of wind speed and sea level pressure simulated by (a) MM5, (b) WRF and (c) COAMPS on 1500 UTC 30 March 2007.

ETA scheme. The MRF scheme, which used a prescribed K profile, is not well behaved for unstable conditions because the scheme cannot handle conditions when atmosphere is well mixed due to the counter-gradient fluxes, whereas the prognostic TKE equation and local vertical mixing in the Eta PBL scheme provided more realistic magnitudes for the eddy exchange coefficients K. Therefore, in the present study, the strong winds above 13 m s^{-1} were better simulated by the ETA scheme, even though the result was slightly influenced by the selection of CP. This result is similar to the simulation result as shown by Braun and Tao (2000). They examined that an excessively deep vertical mixing of the MRF scheme acted to dry the lower PBL and reduce hurricane intensity. In addition, it was shown in the comparison between the results of EXP1 and EXP2 that the Grell CP simulated more realistic magnitude of strong wind speed than Betts-Miller CP.

5. Comparison of three models for cyclone development

To examine the simulations of cyclone development, three runs of MM5 with EXP2, WRF with EXP2 and COAMPS were compared. Surface weather charts and the distribution of wind speed and sea level pressure fields simulated by three models on 1500 UTC 30 March 2007 are shown in Fig. 6. Models simulate the cyclone in the southern part of western Korean Peninsula, and the result shows the anticyclone in the north of the cyclone as shown in the black box of the Fig. 2. The WRF simulated the developed mesoscale cyclone whereas COAMPS shows the cyclone westward from the south-western part of the Korean Peninsula. The WRF model provided the best simulation result of strong wind region around Yeonggwang where was struck by the storm surge (Fig. 6b). This result seems to be related to the differences between MM5 and WRF which are represented by the dynamic frame, horizontal coordinate and the conservative for scalar variables (Table 1).

Figure 7 displays the time series of wind speed and sea level pressure obtained by observation and simulations by MM5, WRF and COAMPS model. The strongest wind speed occurred at 1600 UTC 30 March. Before that maximum peak, wind speed showed a weak peak at 0400 UTC and 0800 UTC 30 March and it fell to zero at 1200 UTC 30 March. Maximum wind speed arrived at 1600 UTC 30 March, showing rapid development with about 12 m s^{-1} speed for five hours. The COAMPS model simulated the evolution but for a smaller magnitude. The WRF and MM5 with EXP2 physics have an early evolution and a delayed maximum magnitude, respectively. As time went on, simulated sea level pressures showed the stronger second peak after the first peak, compared to that of observation. Figure 7a shows that wind speeds of models were underestimated on 1012 UTC and overestimated on 2124 UTC, which was also analyzed by Zhang and Zheng (2004). They showed that the Eta PBL scheme underestimate the strength of surface wind during the daytime and overestimate it at night.

We compared the atmospheric states to investigate

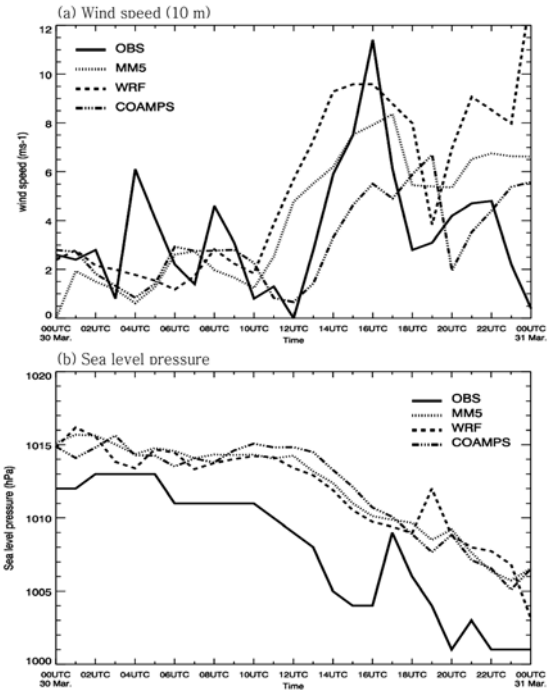

Fig. 7. Temporal variation of (a) wind speed and (b) sea level pressure obtained by observation and simulations with MM5, WRF and COAMPS at Yeonggwang.

the cause of the cyclone development. Low-level warm air advection, convective instability, low-level moisture flux and its convergence and longitude-height cross-section of temperature were investigated.

Figure 8 shows the horizontal distribution of temperature advection at 900 hPa. Figure 8a and Fig. 8b are analysis data from the NCEP Final Analysis (FNL) and Figs. 8c-8h show the simulated temper-

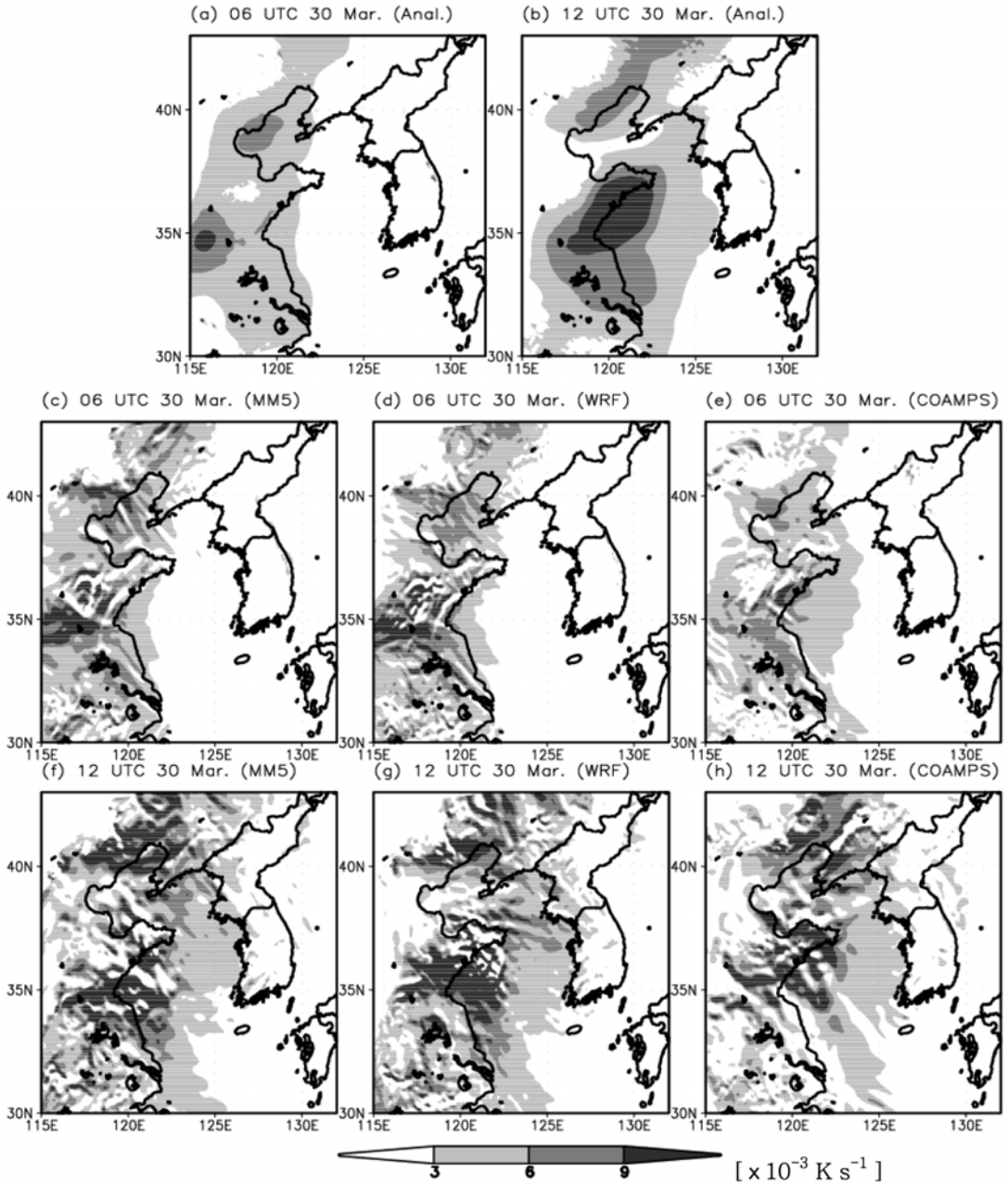

Fig. 8. Horizontal distribution of warm air advection (x 10^{-3} K s^{-1}) at 900 hPa simulated by (a) analysis data on 0600 UTC 30 March 2007, (b) analysis data on 1200 UTC 30 March 2007, (c) MM5, (d)WRF and (e) COAMPS on 0600 UTC 30 March 2007 and (f) MM5, (g)WRF and (h) COAMPS on 1200 UTC 30 March 2007.

ature advection using MM5, WRF and COAMPS. The region of warm advection over 3.0×10^{-3} K s^{-1} is shaded. Analysis data showed that the warm advection region is situated in the eastern part of China with the core (116°E, 35°N) at 0600 UTC 30 March 2007 (Fig. 8a). As time went on, the region of warm advection moved eastward and extended to the broad area. On 1200 UTC 30 March 2007, the warm advection

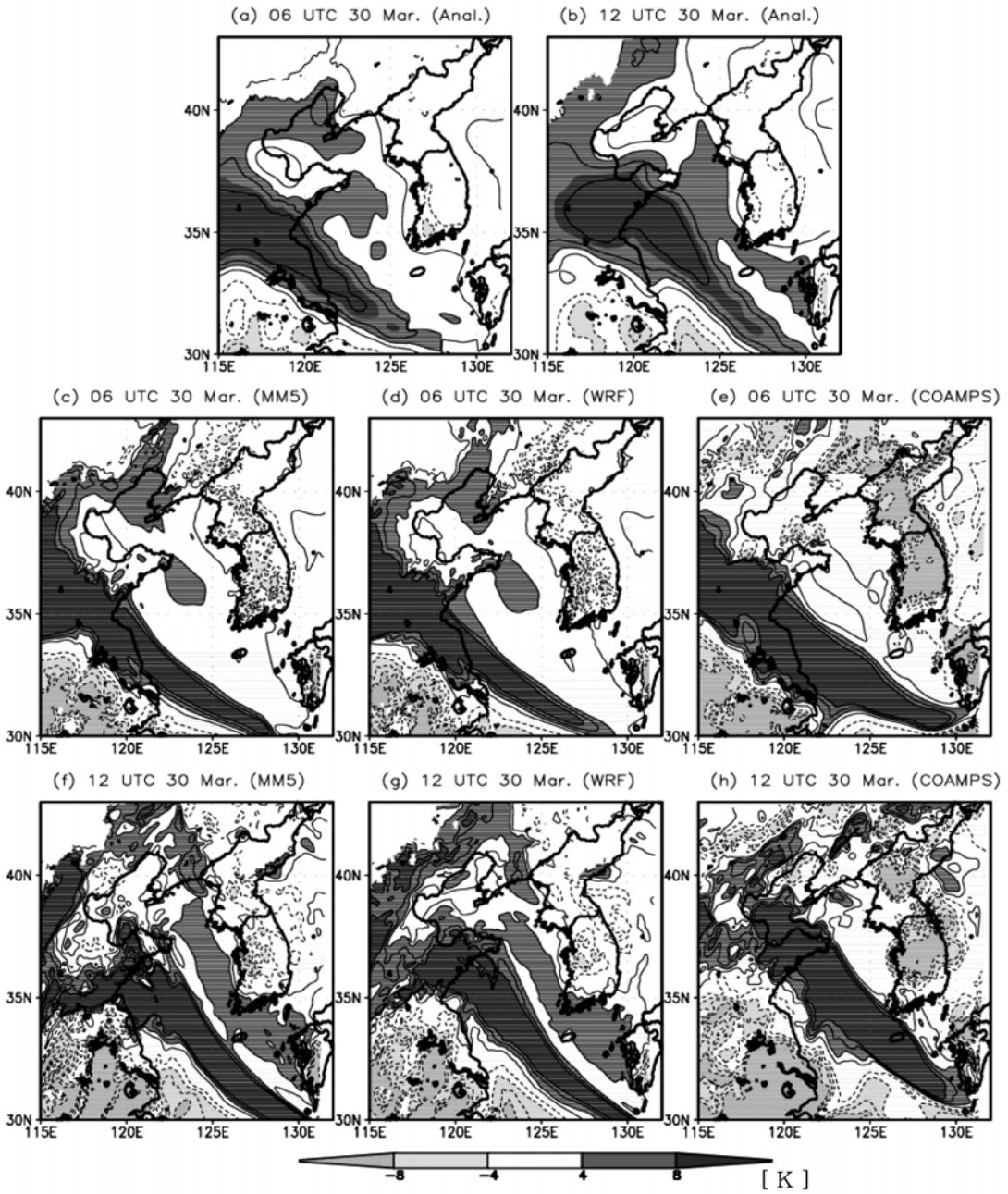

Fig. 9. Same as Fig. 8 except for convective instability (difference between equivalent potential temperature (θ_e) at 850 hPa and θ_e at 900 hPa, K).

arrived in the Korean Peninsula and the core was located at 120.5°E, 35.5°N (Fig. 8b). All models simulated the region of warm advection and the core compared with the analysis data. On 0600 UTC 30 March 2007, COAMPS model showed that the warm advection region was located more eastward to the Korean Peninsula and the core was weaker than MM5 and WRF. We proved that WRF simulated a broad region of warm advection over 9×10^{-3} K s^{-1} compared with MM5 and COAMPS in the Yellow Sea at 1200 UTC

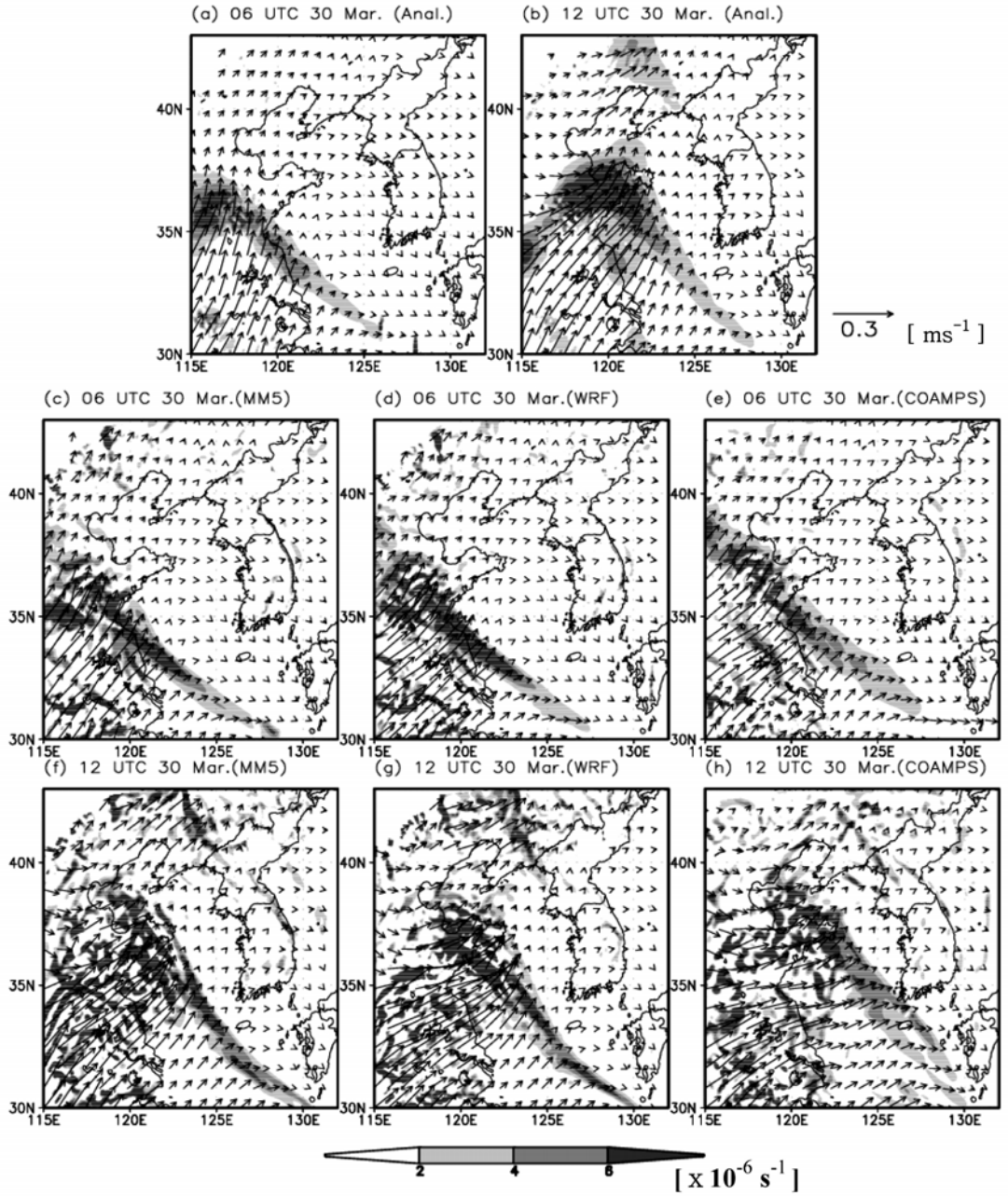

Fig. 10. Same as Fig. 8 except for moisture flux (vector, m s^{-1}) and its convergence (shaded, x 10^{-6} s^{-1}).

30 March 2007.

To measure the convective instability, the gradient between equivalent potential temperature (θ_e) at 900 hPa and θ_e at 850 hPa were calculated (Fig. 9), where the positive value means stable and the negative value means unstable. Analysis data showed that the stable region was located from the eastern part of China to the Yellow Sea and the instable region was located on the southeastern part of China and southwestern part of the Korean Peninsula on 0600 UTC 30 March 2007 (Fig. 9a). As time went on, the pattern moved northeastward and the stable region was destabilized in the Yellow Sea (Fig. 9b). Convective instability fields occurred at the western Korean Peninsula, which corresponded to the area of warm advections downstream. The warm air advection destabilized

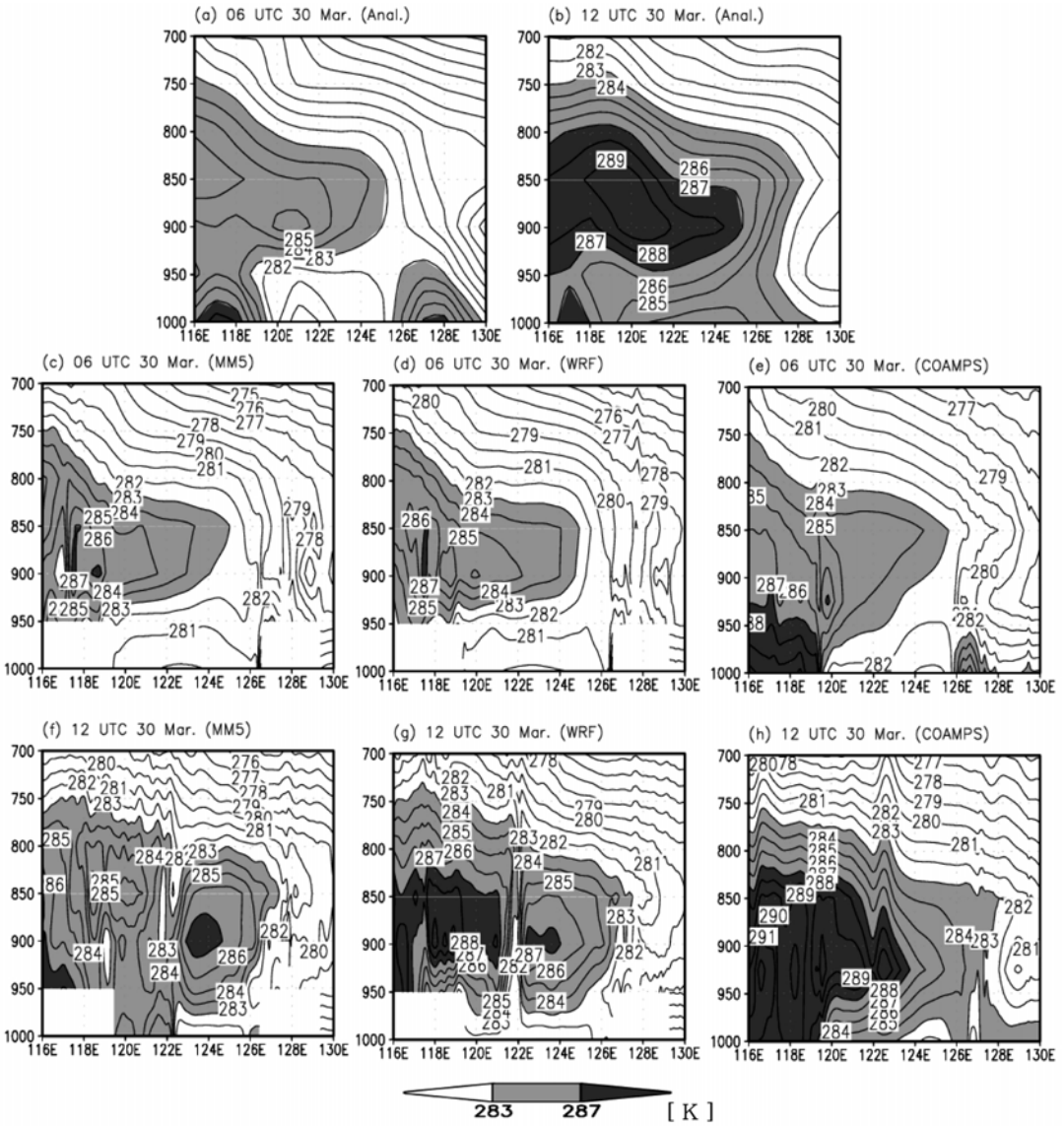

Fig. 11. Longitude-height cross-section of temperature (K) at 35.25°N from 116°E to 130°E simulated by (a) analysis data on 0600 UTC 30 March 2007, (b) analysis data on 1200 UTC 30 March 2007, (c) MM5, (d) WRF and (e) COAMPS on 0600 UTC 30 March 2007 and (f) MM5, (g) WRF and (h) COAMPS on 1200 UTC 30 March.

the low layer from 900 hPa to 850 hPa.

Figure 10 shows the horizontal distribution of moisture flux and its convergence at 900 hPa. Moisture flux and its convergence were calculated by $\mathbf{v} \cdot q$ and $\nabla \cdot (q \cdot \mathbf{v})$, respectively. The region of moisture convergence over 2.0×10^{-6} s^{-1} is shaded. Analysis data showed that the convergence of moisture flux region was situated in the eastern part of the China on 06 UTC 30 March 2007 (Fig. 10a). As time went on, the region of moisture convergence moved northeastward and extended to the broad area. On 1200 UTC 30 March 2007, the convergence of moisture flux region in the NW-SE direction was generated over the Yellow Sea due to the transport of moisture flux from southwest (Fig. 10b). All models simulated the moisture flux and moisture convergence region compared with the analysis data. We showed that MM5 and WRF simulated a broad region of moisture convergence over 6.0×10^{-6} s^{-1} compared with the COAMPS. The strong moisture convergence merged to the warm air advection area. Low-level warm advection destabilized the low-level, and then moisture flux contributed to enhance the development of the cyclone.

We also compared the longitude-height cross-section of temperature at 35.25°N from 116°E to 130°E to analyze the cause of cyclone development (Fig. 11). Almost all of the warm cores existed at 900 hPa. There were two warm cores (116°E-124°E and 126°E-130°E) on 0600 UTC 30 March 2007 and the cores merged and developed on 1200 UTC 30 March 2007 in analysis data. All models simulated the warm core compared with the analysis data, especially in the COAMPS model. On 0600 UTC 30 March 2007, all models had the core from 116°E to 125°E and COAMPS had another core from 126°E to 127.5°E. As time went on, the core was developed and extended eastward.

6. Summary and conclusion

The storm surge on 30 March 2007 was an exceptional one generated by a mesoscale cyclone with a center pressure of 1010 hPa. To predict storm surges, accurate sea level pressures and sea surface winds are required. In this study, the sea level pressure and sea surface wind were simulated with different MM5, WRF and COAMPS and physics options. We selected the physics options as the optimal parameterizations for the high wind conditions and investigated the cause of the cyclone development.

At first, EXP1 (Eta PBL and Betts-Miller cumulus), EXP2 (Eta PBL and Grell cumulus), EXP3 (MRF PBL and Kain-Fritsch cumulus) with MM5 and WRF were designed for optimal combination of physics. EXP2 and EXP3 show better distributions of strong wind speed regions compared to EXP1. Although there is some difficulty in selecting the optimal physics options, EXP2 showed good performance in terms of the distribution and the magnitude of wind speed, especially in the case of strong wind.

We showed that different models make much difference in the magnitude and the evolution of a cyclone. The results for three runs of MM5 with EXP2, WRF with EXP2 and COAMPS showed that the distribution of wind speed corresponds well to sea level pressure. The WRF and MM5 with EXP2 physics have an early evolution and a delayed maximum magnitude respectively, while the COAMPS model simulated the evolution but for a smaller magnitude.

The causes of cyclone development are considered to be warm advection, moisture flux and its convergence, and convective instability. The results of the numerical simulations performed in this study showed that WRF simulated the developed mesoscale cyclone. WRF simulation is stronger than MM5 and COAMPS in the western Korean Peninsula in terms of warm advection and moisture convergence. Low-level warm advection destabilized the low-level, and then moisture flux contributed to enhance the development of the cyclone. Because this study is based on the result for one case, further study with more cases will be required to understand and simulated the high-wind conditions.

Acknowledgement. This work was supported by Top-Brand project of KORDI and Pusan National University Research Grant (2006). This work was also supported by the Brain Korea 21 Project in 2006/7.

REFERENCE

Betts, A. K., 1986: A new convective adjustment scheme. Part I: Observational and theoretical basis. *Quart. J. Roy. Meteor. Soc.*, **112**, 677-691.

_____, and M. J. Miller, 1993: The Betts-Miller scheme. *The representation of cumulus convection in numerical models*. Eds., Amer. Meteor. Soc., 246pp.

Braun, S. A., and W.-K. Tao, 2000: Sensitivity of high-resolution simulations of Hurricane Bob (1991) to planetary boundary layer parameterizations. *Mon. Wea. Rev.*, **128(12)**, 3941-3961

Chen, S. -J., and L. Dell'osso, 1987: A numerical case study of East Asian coastal cyclogenesis. *Mon. Wea. Rev.*, **115**, 477-487.

Davis, C. A., and S. Low-Nam, 2001: The NCAR-AFWA tropical cyclone bogussing scheme. *A Report Prepared for the Air Force Weather Agency (AFWA)*, National Center for Atmospheric Research, Boulder, Co., 13pp.

Dudhia, J., 1989: Numerical study of convection observed during the winter monsoon experiment using a mesoscale two-dimensional model. *J. Atmos. Sci.*, **46,** 3077-3107.

Grell, G. A., J. Dudhia, and D. R. Stauffer, 1994: *A description of the fifth generation Penn State/NCAR Mesoscale Model (MM5)*. NCAR Tech. Note, NCAR/TN-398+ STR, 121pp.

Hong, S.-Y., and H.-L. Pan, 1996: Nocturnal boundary layer vertical diffusion a medium-range forecast model. *Mon. Wea. Rev.*, **124**, 2322-2339.

Ivanov, S., and Y. Palamarchuk, 2007: Systematic error of parameterization schemes in the MM5 model. *Proceedings of The 3rd WGNE Workshop on Systematic Errors in Climate and NWP Models*, 12-16 February, San Francisco, 49pp.

Janjic, Z. I., 1990: The step-mountain coordinate: physical package. *Mon. Wea. Rev.*, **118**, 1429-1443.

_____, 1994: The step-mountain eta coordinate model: further developments of the convection, viscous sublayer and turbulence closure schemes. *Mon. Wea. Rev.*, **122**, 927-945.

Joung, C.-H., S. S. Kim, S.-U. Park, K. D. Min, and H. -S. An, 1984: A case study on the extratropical cyclone development on the East Sea. *J. Korean Meteor. Soc.*, **20**, 1-21. (in Korean with English abstract)

Kain, J. S., and J. M. Fritsch, 1993: Convective parameterization for mesoscale models: The Kain-Fritsch scheme. *The representation of cumulus convection in numerical models*. Eds., Amer. Meteor. Soc., 246pp.

Lee, D.-G., C.-H. Joung, S.-U. Park, S.-C. Yoon, C.-W. Lee, Y.-H. Kuo, and S. Low-Nam, 1991: Numerical simulations of an explosive cyclogenesis near the East Asian coast. *J. Korean Meteor. Soc.*, **27**, 1-20. (in Korean with English abstract)

_____, and D.-E. Chang, 1997: Sensitivity of cyclone development to initial data using an adjoint model. *J. Korean Meteor. Soc.*, **33**, 363-384. (in Korean with English abstract)

_____, and S.-Y. Hong, 1989: A case study of the sensitivity of sea surface temperature on the mesoscale model simulation of winter cyclone development. *J. Korean Meteor. Soc.*, **25**, 1-14. (in Korean with English abstract)

Mellor, G. L., and T. Yamada, 1982: Development of a turbulence closure model for geophysical fluid problems. *Rev. Geophys.*, **20**, 851-875.

Mlawer, E. J., S. J. Taubman, P. D. Brown, M. J. Iacono, and S. A. Clough, 1997: Radiative transfer for inhomogeneous atmosphere: RRTM, a validated correlated-k model for the longwave. *J. Geophys. Res.*, **102**, 16663-16682.

Orlanski, I., and J. J. Katzfey, 1987: Sensitivity of model simulations for a coastal cyclone. *Mon. Wea. Rev.*, **115**, 2792-2821.

Reisner, J. R., R. M. Rasmussen, and R. T. Bruintjes, 1998: Explicit forecasting of supercooled liquid water in winter storms using the MM5 mesoscale model. *Quart. J. Roy. Meteor. Soc.*, **124**, 1071-1107.

Zhang, D.-L., and W.-Z. Zheng, 2003: Diurnal cycles of surface winds and temperatures as simulated by five boundary-layer parameterizations. *J. Appl. Meteorol.*, **43(1)**, 157-169.